at low water content is ~1, in agreement with sorption data (column B, Table I) and at full hydration is only ~7. However, at intermediate levels of hydration the selectivity peaks at ~47. It appears that at this level of hydration the water sheath adhering to the zeolite channels has optimized this dimension for selection between the olefins.[11]

These observations suggest, therefore, that the dichotomy between columns B and C of Table I is best explained in terms of the effect of the residual water content of the catalysts (Table I, column G) in modifying the framework size selectivity.[12] This latter observation indicates that a delicate balance exists between selectivities based on pore size and on moisture content. This situation probably occurs in any catalytic system employing a zeolite (particularly when water is a byproduct of the catalytic reaction) and the marked contribution of moisture content toward catalytic selectivity should not be overlooked.

Acknowledgment. The authors thank Dr. P. E. Bierstedt for the XPS measurements and J. B. Jensen, G. F. Diffendall, W. B. Arters, and R. W. Shiffer for technical assistance. We also thank Dr. J. Schwartz for helpful discussions and advice on the preparation of the Rh–allyl–X catalyst.

Registry No. Rh, 7440-16-6; tris(π-allyl)rhodium, 12082-48-3.

(11) An alternative interpretation for this observed effect of water content might consider the water to be modifying the active rhodium sites by coordination. This effect has been shown by Rylander: Rylander, P. L. "Catalytic Hydrogenation over Platinum Metals"; Academic Press: New York, 1967; p 328. While this type of effect may contribute to altered selectivities, we feel that the appearance of a maximum in, and the general shape of, the selectivity curve (Figure 2) is better explained if the proposed mechanism of pore size modification is the major contributor to selectivity. Experiments to clarify this point further will be performed in these laboratories.

(12) Breck, D. W. "Zeolite Molecular Sieves"; Wiley: New York, 1974; pp 644-45.

Contribution from the Department of Chemistry, Washington State University, Pullman, Washington 99164-4630

Reduction Potential and Bonding Trends in Manganese(I) and Manganese(II) Hexakis(aryl and alkyl isocyanides)

ROGER M. NIELSON and SCOT WHERLAND*

Received September 7, 1984

This paper presents infrared, Raman, and cyclic voltammetry results on $Mn(CNR)_6BF_4$ and $Mn(CNR)_6(BF_4)_2$ complexes, where R is methyl, ethyl, isopropyl, *tert*-butyl, cyclohexyl, benzyl, phenyl, *p*-tolyl, and *p*-anisyl. These results are interpreted with the aid of self-consistent field ab initio calculations (GAUSSIAN 76) on the ligands. The $E_{1/2}$ values correlate well with the energy calculated for the lowest energy π^* orbital of the ligands. It is concluded that the $E_{1/2}$ values reflect the HOMO energy of the complexes. The back-bonding is further probed by using the observed trends in the apparent MnC and CN force constants. It is concluded that the CN force constants and vibrational frequencies are not good measures of the back-bonding interaction when alkyl and aryl isocyanide complexes are being compared because of the delocalized nature of the HOMO in the aromatic case.

Introduction

We became interested in manganese isocyanide complexes because of their electron-transfer reactivity. We have previously investigated the effect of solvent and added salt on the electron self-exchange reaction

$$Mn(CNR)_6^+ + Mn(CNR)_6^{2+} \rightleftharpoons Mn(CNR)_6^{2+} + Mn(CNR)_6^+$$

in which R is cyclohexyl,[1] and in acetonitrile only we have investigated the effect of varying the R group over the range methyl, ethyl, isopropyl, *tert*-butyl, and benzyl.[2] The first study generally showed a lack of correlation with the solvent dielectric continuum theory of solvent reorganization and established the effect of ion pairing as distinct from the effect of ionic strength. The second study demonstrated a decrease in electron-transfer rate constant with increasing ligand bulk. This is the best example of such an effect in bimolecular chemistry. The benzyl isocyanide complex exhibited a somewhat higher reactivity than would be predicted from its size. Studies currently in progress on phenyl, *p*-tolyl, and *p*-anisyl isocyanide complexes demonstrate a greatly enhanced reactivity compared to alkyl ligands of similar size. The most obvious interpretation of the enhanced reactivity for the phenyl series, and possibly the benzyl compound, is that π bonding allows electron density from the manganese nucleus to be delocalized onto the ligand, thus effectively decreasing the electron-transfer distance.

In order to further characterize these compounds and investigate the extent of delocalization, we have made a series of physical measurements. These include ^{55}Mn, ^{14}N, ^{13}C, and ^1H NMR, EPR, room-temperature solution and solid-state magnetic susceptibility, infrared, Raman, ultraviolet spectroscopy, cyclic voltammetry, and several ab initio molecular orbital (MO) calculations on the ligands alone.

Some spectroscopic, electrochemical,[3,4] and quantum-mechanical calculation data[5,6] are available in the literature for these complexes. These data are limited to some ^1H[7] and ^{14}N NMR[8] data, EPR,[7,9] ultraviolet absorption measurements,[6,10] infrared data[11] on most of the complexes, and Raman data for the methyl and phenyl isocyanide complexes.[12] Of these data, we have been unable to reproduce the EPR and ^1H NMR results for the Mn(II) complexes, as discussed elsewhere.[13]

Our results on the physical properties have been divided into two reports. This paper discusses the Raman, infrared, cyclic

(1) Nielson, R. M; Wherland, S. *Inorg. Chem.* **1984**, *23*, 1338.
(2) Nielson, R. M.; Wherland, S. *J. Am. Chem. Soc.* **1985**, *107*, 1505.
(3) Treichel, P. M.; Mueh, H. J. *Inorg. Chem.* **1977**, *16*, 1167.
(4) Gritzner, G. *Monatsh. Chem.* **1976**, *107*, 1499.
(5) Sarapu, A. C.; Fenske, R. F. *Inorg. Chem.* **1975**, *14*, 247.
(6) Fantucci, P. C.; Valenti, V.; Cariati, F. *Inorg. Chim. Acta* **1971**, *5*, 425.
(7) Fantucci, P. C.; Naldini, L.; Cariati, F.; Valenti, V. *J. Organomet. Chem.* **1974**, *64*, 109.
(8) Becker, W.; Beck, W.; Rieck, R. *Z. Naturforsh., B: Anorg. Chem., Org. Chem., Biochem., Biophys., Biol.* **1970**, *25B*, 1332.
(9) Matteson, D. S.; Bailey, R. J. *J. Am. Chem. Soc.* **1969**, *91*, 1975.
(10) Mann, K. R.; Cimolino, M.; Goeffroy, G. L.; Hammond, G. S.; Orio, A. A.; Albertin, G.; Gray, H. B. *Inorg. Chim. Acta* **1976**, *16*, 97.
(11) Cotton, F. A.; Zingales, F. *J. Am. Chem. Soc.* **1961**, *83*, 351.
(12) Verndonck, L.; Tulun, T.; Van der Kelen, G. P. *Spectrochim. Acta, Part A* **1979**, *35A*, 867.
(13) Nielson, R. M.; Wherland, S. *Inorg. Chem.*, in press.

0020-1669/85/1324-1803$01.50/0

voltammetry, and MO calculations and some bonding trends for several Mn^{I}- and $Mn^{II}(CNR)_6$ complexes where R = methyl, ethyl, isopropyl, *tert*-butyl, cyclohexyl, benzyl, phenyl, *p*-tolyl, and *p*-anisyl. The companion paper presents the multinuclear NMR, a discussion of the EPR, and magnetic susceptibility results for both the Mn(I) and Mn(II) complexes.[13]

Experimental Section

The manganese isocyanide complexes were prepared and acetonitrile and nitrobenzene were dried, as previously described.[1,14] Nitromethane and dichloromethane were stirred over Drierite for 2 days and then fractionally distilled through a 70-cm Vigreux column from fresh Drierite. Raman spectra were collected at room temperature for solid and solution samples of the Mn(I) complexes, and for solid samples of the Mn(II) complexes, in capillary tubes, with a Ramanor HG25 instrument. For the solution Mn(I) and the solid Mn(II) samples, the red 6471-Å line of a krypton ion laser was used, and for the solid Mn(II) and solution Mn(I) samples, the green 5145-Å of an argon ion laser was used. Data were collected in the 100–3500-cm^{-1} region, with four scans being averaged. Polarization experiments were performed on the solution samples by using a polarization analyzer in the laser beam. The optimum horizontal polarization of the analyzer was obtained by minimizing the intensity of the CN A_{1g} band. The totally symmetric polarized spectrum was obtained by multiplying the spectrum obtained with the light polarized in the horizontal plane by $^{7}/_{6}$ and subtracting this value from the spectrum obtained with the light polarized in the vertical plane. The instability of the solutions to the laser source required that fresh, bubble-free solution be continually pumped through the capillary sample tube at a rate of 1 mL/min.

Infrared spectra were collected with a Perkin-Elmer 283-B instrument in the 4000–250-cm^{-1} region. The spectra of the Mn(I) samples were collected as KBr pellets, and the spectra of the Mn(II) samples, as Nujol mulls due to reduction of the Mn(II) complex by bromide.

Electrochemical measurements were performed at room temperature with a Princeton Applied Research Model 303 cell assembly and an MPI Model MP 1502B voltammetry controller adapted for *ir* compensation. A three-electrode system was used employing platinum working and counter electrodes and an isolated silver reference electrode. The cyclic voltammograms were digitized, and the anodic and cathodic peaks were fit in the smoothed data. Decamethylferrocene (Strem Chemicals, Inc.) was used as an internal standard to eliminate junction potential effects. Concentrations of the complexes and the internal standard were 1 mM, and the concentration of the inert electrolyte (tetrabutylammonium tetrafluoroborate) was 0.10 M. Each measurement was taken three times with fresh solution.

A Perkin-Elmer Model 320 spectrophotometer was used in the collection of the room-temperature electronic absorption spectra. The solvent was acetonitrile, and 1-cm cells were used.

The ab initio MO calculations were performed on an Amdahl 470V/8 computer at the Washington State University Computing Service Center using the GAUSSIAN 76 programs.[15] The electronic structure of methyl isocyanide was calculated with several basis sets ranging from the minimal STO-2G to the more complex STO-6-31G**, and the results were compared to the experimental ionization potentials[16] and dipole moment.[17] Taking into consideration both the accuracy of the results and the amount of computation time for each basis set, the basis set STO-4-31G was chosen for the calculations. Unfortunately, the memory requirements were too great to permit this basis set to be used for the cyclohexyl, benzyl, *p*-tolyl, and *p*-anisyl isocyanides, so for these molecules the basis set STO-6G was used. The reported energy values for the calculations performed with the STO-6G basis were "normalized" to correspond to the magnitude of the values obtained from the STO-4-31G results. This normalization procedure merely consisted of performing the MO calculations for the methyl, ethyl, isopropyl, *tert*-butyl, and phenyl isocyanides with both the STO-4-31G and the STO-6G basis sets and then comparing the energy differences between the results of the two calculations for the same MO. An average energy difference was computed, and this value was subtracted from the energies of the MO's from the calculations with the STO-6G basis set. The trends in the energy values were not sensitive to this procedure since the difference in MO energies was appreciable between the isocyanides. Experimental geometries are not known for all the isocyanides, so the experimental geometry of methyl isocyanide[18] was used as a standard for the alkyl ligands and the crystal for $Mn(CNC_6H_5)I_3$[19] was used as a standard for the geometry of the molecules containing aromatic rings. The bond lengths, angles, and the *x*, *y*, *z* coordinates for the isocyanide molecules are given in the supplementary material. The advantage of using the same bond lengths and angles in the molecules is that any trends observed in the MO energies will be due to electronic effects and not to bond length changes.

Results

Since we are primarily concerned with the metal–ligand bond and the CN triple bond, we report the vibrational frequencies associated with these bonds only. The complete Raman spectra are available as supplementary material. Assuming that the manganese isocyanide complexes are locally octahedral, the MnC and CN stretching vibrations will transform as A_{1g}, E_g, and T_{1u}, of which T_{1u} is infrared active and A_{1g} and E_g are Raman active. The A_{1g} bands are polarized and are therefore separable from the E_g bands. The assignment of the MnC A_{1g} absorption was based on its polarized nature and low frequency. This assignment was unambiguous for all except the cyclohexyl complexes. The MnC E_g and T_{1u} assignments were not made and are unimportant for this work. Assignment of the CN A_{1g}, E_g, and T_{1u} bands was obvious in all the complexes since these are the most intense bands in the spectrum. For the Mn(I) complexes the CN E_g band was much more intense than the A_{1g} mode while these two bands were of nearly equal intensity for the Mn(II) complexes. The CN T_{1u} band for the Mn(II) complexes was sharp, but for the Mn(I) complexes the band was broad and had a shoulder on the low-energy side for all except the methyl and ethyl complexes. The results of the Raman and infrared experiments are given in Table I and agree with prior measurements where comparisons can be made.[11,12]

We have calculated force constants for the MnC and the CN vibrations since they are more indicative of bond strength than are the vibrational frequencies. For the CN force constants, we used the Cotton–Kraihanzel (CK)[20] method as used previously for $Mn(CNCH_3)_6^{+}$.[5] The CK method equations (1a)–(1c) for

$$\lambda_{A_{1g}} = \mu(k + 6k_i) \tag{1a}$$

$$\lambda_{E_g} = \mu k \tag{1b}$$

$$\lambda_{T_{1u}} = \mu(k - 2k_i) \tag{1c}$$

calculating the force constants from the individual vibration frequencies are given where λ_i is the product of 5.8890×10^{-2} and the square of the appropriate vibration frequency (cm^{-1}), μ is the reciprocal of the reduced mass of the CN group, k is the vibration force constant, and k_i is the stretch–stretch interaction constant. For the MnC and the free-ligand CN vibrations, eq 2 was used,[21] where ν is the frequency of the vibration for the

$$k = (5.8890 \times 10^{-2})\nu^2 m \tag{2}$$

totally symmetric stretch mode and m is the mass of the entire isocyanide ligand for the calculations of the complexes and the reduced mass of the CN group for the free-ligand calculations. Table I also contains the calculated force constants for the MnC and CN bonds from eq 2 for k_{MnC}, eq 1a for $k_{i(CN)}$, and eq 1b for k_{CN}.

The data in Table I show that the MnC force constants are smaller for the Mn(II) complexes than for the Mn(I) complexes. The CN force constants are larger for the Mn(II) complexes than for the Mn(I), and the force constants for the free-ligand value fall between those for the Mn(I) and Mn(II) complexes.

The results of the cyclic voltammetry experiments are given in Table II. The trends in the $E_{1/2}$ values compare well to earlier

(14) Borchardt, D.; Wherland, S. *Inorg. Chem.* **1984**, *23*, 2537.
(15) Hehre, W. J.; Latham, W. A.; Ditchfield, R.; Newton, M. D.; Pople, J. A. *QCPE* **1976**, *368*.
(16) Turner, D. W.; Baker, C.; Baker, A.; Brundle, C. K. "Molecular Photoelectron Spectroscopy"; Wiley-Interscience: New York, 1970; p 347.
(17) Ghosh, S. N.; Trambarulo, R.; Gordy, W. *J. Chem. Phys.* **1953**, *21*, 308.
(18) Sutton, L. E. "Tables of Interatomic Distances and Configurations in Molecules and Ions, Supplement"; Chemical Society: London, 1965.
(19) Ericsson, M. S.; Jagner, S.; Ljunstrom, E. *Acta Chem. Scand., Ser. A* **1980**, *A34*, 535.
(20) Cotton, F. A.; Kraihanzel, C. S. *J. Am. Chem. Soc.* **1962**, *84*, 4427.
(21) Li, T. T. T.; Weaver, M. J.; Brubaker, C. H., Jr. *J. Am. Chem. Soc.* **1982**, *104*, 2381.

Table I. MnC and CN Vibrational Frequencies (cm^{-1}) and Force Constants (mdyn/Å) for $Mn(CNR)_6BF_4$ and $Mn(CNR)_6(BF_4)_2$

	Mn—C		C≡N					free ligand	
	$\nu_{A_{1g}}$	k_{MnC}	$\nu_{A_{1g}}$	ν_{E_g}	$\nu_{T_{1u}}$	k_{CN}	$k_{i(CN)}$	ν_{fl}[a]	$k_{CN,lig}$
$Mn(CNCH_3)_6BF_4$	292	2.06	2210	2142	2114	17.47	0.19	2165	17.85
$Mn(CNCH_3)_6(BF_4)_2$	270	1.76	2255	2233	2214	18.99	0.16		
$Mn(CNC_2H_5)_6BF_4$	267	2.31	2190	2126	2084	17.21	0.18	2151	17.61
$Mn(CNC_2H_5)_6(BF_4)_2$	231	1.73	2241	2217	2194	18.72	0.19		
$Mn(CNC_3H_7)BF_4$	225	2.06	2187	2111	2104[c]	16.97	0.21	2144	17.50
					2039 sh				
$Mn(CNC_3H_7)_6(BF_4)_2$	200	1.63	2232	2205	2194	18.51	0.09		
$Mn(CNC_4H_9)_6BF_4$	196	1.88	2178	2104	2094[c]	16.86	0.20	2137	17.39
					2049				
$Mn(CNC_4H_9)_6(BF_4)_2$	170	1.42	2218	2196	2176	18.36	0.16		
$Mn(CNC_6H_{11})_6BF_4$	216 (173)[b]	3.00 (1.93)	2181	2106	2079[c]	16.89	0.20	2140	17.44
					2049 sh				
$Mn(CNC_6H_{11})_6(BF_4)_2$	183	2.15	2226	2202	2191	18.46	0.09		
$Mn(CNCH_2C_6H_5)_6BF_4$	190	2.49	2206	2130	2104[c]	17.28	0.21	2146	17.54
					1917 sh				
$Mn(CNCH_2C_6H_5)_6(BF_4)_2$	181	2.26	2244	2215	2194[c]	18.68	0.19		
					2189				
$Mn(CNC_6H_5)_6BF_4$	171	1.78	2184	2109	2084	16.94	0.20	2127	17.22
$Mn(CNC_6H_5)_6(BF_4)_2$	*d*	*d*	*d*	*d*	2154	17.96[g]	0.15[f]		
$Mn(CNC_6H_4CH_3)_6BF_4$[e]			2184	2110	2086	16.95	0.19	2126	17.21
$Mn(CNC_6H_4CH_3)_6(BF_4)_2$[e]					2162	18.10[g]	0.15[f]		
$Mn(CNC_6H_4OCH_3)_6BF_4$[e]			2179	2114	2088	17.02	0.21	2126	17.21
$Mn(CNC_6H_4OCH_3)_6(BF_4)_2$[e]					2157	18.02[g]	0.15[f]		

[a] Fl = free ligand. Infrared-active band of the free ligand taken from: Stephany, R. W.; deBie, M. J. A.; Drenth, W. *Org. Magn. Reson.* **1974**, *6*, 45. [b] Two polarized bands were obtained in the low wave number region, and the MnC A_{1g} could not be positively identified. [c] The higher value is the peak maximum, and the lower value is the shoulder position. [d] Raman data could not be obtained due to the absorption of the laser light and decomposition of the sample. [e] The Raman and infrared data for these complexes were taken from ref 7. [f] This is the average of $k_{i(CN)}$ for the other complexes. [g] This value was calculated from eq 1 with the average value of $k_{i(CN)}$ for the other complexes.

Table II. Reduction Potential Data (mV) for $Mn(CNR)_6BF_4$ with Respect to Ferrocene[a]

R	$E_{1/2}$ (CH_3CH)[b]	$E_{1/2}$ (CH_2Cl_2)[b]	$E_{1/2}$ (CH_3NO_2)[b]	$E_{1/2}$ $(PhNO_2)$[b]
CH_3	3	−34	−2	−30
CH_3CH_2	8			
$CH(CH_3)_2$	30			
$C(CH_3)_3$	43	60	30	46
C_6H_{11}	57			
$CH_2C_6H_5$	189	159	190	172
C_6H_5	455			
$C_6H_4CH_3$	391			
$C_6H_4OCH_3$	315			

[a] The potential of ferrocene vs. saturated calomel is 310 mV in acetonitrile: Mann, C. K.; Barnes, K. K. "Electrochemical Reactions in Nonaqueous Systems"; Marcel Dekker: New York, 1970; pp 403–446. The potential of ferrocene vs. decamethylferrocene was determined to be as follows (mV, solvent): 503, acetonitrile; 546, methylene chloride; 509, nitromethane; 521, nitrobenzene. [b] Solvent donor numbers and dielectric constants: CH_3CN, 14.1, 37; CH_2Cl_2, 0, 9; CH_3NO_2, 2.7, 35; $PhNO_2$ 4.4, 39. Gutman, V. *Chim.* **1977**, *31*, 1.

studies,[3,4] where comparisons can be made, except for the benzyl complex. The values are consistently about 65 mV more negative than the literature values, which can be attributed to junction potential differences. Our results for the benzyl complex give an $E_{1/2}$ value about 140 mV more positive than reported, and repeated experiments on well-recrystallized samples were consistent.

$E_{1/2}$ values were determined for all the complexes in acetonitrile and in methylene chloride, nitromethane, and nitrobenzene for the methyl, *tert*-butyl, and benzyl complexes only. The results in Table II indicate an increase in the reduction potential in the order methyl < ethyl < isopropyl < *tert*-butyl < cyclohexyl < benzyl < *p*-anisyl < *p*-tolyl < phenyl in acetonitrile, and for the other solvents the value of $E_{1/2}$ increases in the order methyl < *tert*-butyl < benzyl.

The results of the ab initio MO calculations for the energies of the π antibonding orbitals and the lone-pair orbital are given in Table III and the wave functions obtained for the π antibonding orbitals are given in the supplementary material. Few ab initio calculations have been reported for the isocyanide molecules, but our results compare well with the data that have been reported.[22]

Table III. Energies (eV) of the CN Antibonding Orbitals and the Lone-Pair Orbitals for the Isocyanide Ligands

ligand	π_x^*	π_y^*	lone pr	lone-pr overlap popln
$CNCH_3$	5.644	5.644	−12.48	−0.008
CNC_2H_5	5.411	5.627	−12.47	−0.060
CNC_3H_7	5.342	5.677	−12.48	−0.059
CNC_4H_9	5.633	5.633	−12.50	−0.073
CNC_6H_{11}	4.606	9.669	−12.48	−0.075
$CNCH_2C_6H_5$	3.608	5.777	−12.55	−0.132
CNC_6H_5	2.890	5.675	−12.68	−0.063
$CNC_6H_4CH_3$	3.008	5.764	−12.59	−0.166
$CNC_6H_4OCH_3$	3.226	5.827	−12.53	−0.059

Two antibonding MO's were obtained corresponding to the p_x and p_y orbitals in the CN group where the x direction has been defined as out of the plane of the molecule. The π_x^* and π_y^* orbitals are nearly degenerate for most of the alkyl ligands, but the π_x^* orbital is more stabilized with respect to the π_y^* orbital for the cyclohexyl ligand and the ligands containing aromatic rings. The stabilized nature of one π^* orbital over the other has been noted before for the substituted aromatic isocyanides.[23] The energy of the lone-pair orbitals is essentially constant for all the ligands, with the aromatics being slightly more stabilized. The Mulliken overlap populations in the CN region of the ligand are also presented in Table III for the lone-pair orbital. The populations are slightly negative for all the molecules.

The electronic absorption data for the Mn(I) alkyl complexes consisted of an intense charge-transfer band with two very weak shoulders on the low-energy side. The two shoulders could only be resolved in the derivative spectra. These weak bands have been previously assigned as d–d transitions.[6] The spectra for the aromatic complexes consisted of five intense bands and have been previously assigned to charge-transfer and intraligand transitions.[10]

(22) Ha, T. K. *J. Mol. Struct.* **1972**, *11*, 185. Howell, J. A. S., Saillard, J. Y.; Beuze, A. L.; Jaouen, G. *J. Chem. Soc., Dalton Trans.* **1982**, 2533. Moffat, J. B. *J. Am. Chem. Soc.* **1982**, *104*, 3949. Moffat, J. B. *J. Mol. Struct.* **1984**, *108*, 293. Moffat, J. B. *J. Mol. Struct.* **1978**, *44*, 237.
(23) Bursten, B. E.; Fenske, R. F. *Inorg. Chem.* **1977**, *16*, 963.
(24) Peover, M. E. *Electroanal. Chem. Interfacial Electrochem.* **1967**, *2*, 1.

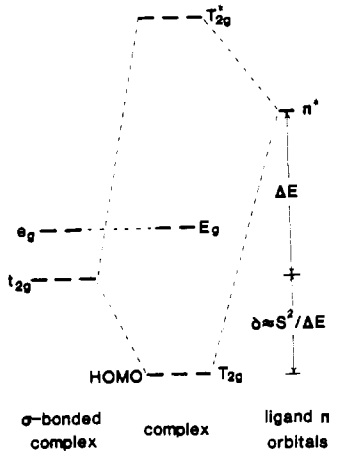

Figure 1. Simple MO diagram describing the bonding between manganese and isocyanide ligands. S represents the overlap integrals between the Mn t_{2g} orbitals and the ligand π^* orbitals. ΔE is the difference in energy between the metal t_{2g} and ligand π^* orbitals.

The data obtained for both the alkyl and the aromatic complexes agreed well with literature values and are not reported further or discussed here.

Discussion

The bonding between the manganese and the isocyanide ligand can be described by a σ-bonding and a π-back-bonding process whereby the ligand donates electron density to the metal through orbitals of σ symmetry and the metal donates electron density back to the ligand through metal t_{2g} orbitals and ligand π-antibonding orbitals. The back-bonding can be described by a very simple MO diagram (Figure 1), where the left side of the diagram shows the energy levels of the metal 3d orbitals split into e_g and t_{2g} components due to the σ bonding to the ligand and the right side of the diagram shows the energy levels of the ligand π-antibonding orbitals. The π^* orbitals are virtual and have a lower electronegativity than the positively charged metal. Hence, these lie higher in energy than the metal 3d orbitals. When back-bonding occurs between the metal t_{2g} and ligand π^* orbitals, two new MO's form, a bonding MO with a lower energy than the metal t_{2g} orbital and an antibonding orbital higher in energy than the ligand π^* orbitals. The new bonding MO will be the HOMO of the complex since the manganese(I) isocyanides are d^6 low-spin complexes. The amount of energy by which the HOMO is stabilized with respect to the metal orbitals is predicted by perturbation theory to be proportional to the square of the overlap integrals between the metal t_{2g} and ligand π^* orbitals divided by the energy difference between them. The overlap integrals will be essentially contant for a series of similar complexes; thus, the energy of the HOMO will decrease as the energies of the metal t_{2g} and ligand π^* orbitals become comparable.

A common method for determining the importance of back-bonding in transition-metal isocyanide complexes is to compare the CN vibration frequencies of the free ligand to those of the metal complex.[11] A decrease in this frequency upon coordination to the metal is taken to indicate that back-bonding is occurring since electrons are being donated from the metal to the ligand π^*-antibonding orbitals, and this decreases the CN bond strength. A better indicator of bond strength is the force constant for the vibration. Table IV gives the difference between the free-ligand CN force constant and that for the Mn(I) and Mn(II) complexes. The positive values for the Mn(I) complexes indicate that back-bonding is occurring, and some trends are apparent. For the Mn(I) alkyls, the difference values increase in the order methyl < ethyl < isopropyl < *tert*-butyl < cyclohexyl, and this indicates that back-bonding also increases in this order. For the complexes containing aromatic rings the difference values indicate that back-bonding increases in the order *p*-anisyl < *p*-tolyl = benzyl < phenyl. The values in Table IV for the Mn(I) complexes, taken alone, indicate that back-bonding is less important for the complexes with aromatic ligands than those with alkyl ligands. This

Table IV. Difference in CN Force Constants between the Free Ligand and the $Mn^{I,II}(CNR)_6(BF_4)_{1,2}$ Complexes

	Δk			Δk	
R	Mn(I)	Mn(II)	R	Mn(I)	Mn(II)
CH_3	0.38	−1.14	$CH_2C_6H_5$	0.26	−0.92
C_2H_5	0.40	−1.11	C_6H_5	0.28	−0.74
C_3H_7	0.53	−1.01	$C_6H_4CH_3$	0.26	−0.89
C_4H_9	0.53	−0.97	$C_6H_4OCH_3$	0.19	−0.81
C_6H_{11}	0.55	−1.02			

contradicts other evidence that suggests that the aromatic complexes have a greater π-acceptor ability than the alkyls.[10,11] For example, $Cr(CNC_6H_5)_6$ is a stable complex, but the corresponding alkyl complexes are less stable. This is presumably due to the greater π-accepting ability of phenyl isocyanide compared to alkyl isocyanides, which leads to stabilization of the Cr through removal of electron density. Infrared data also suggest that back-bonding is more extensive for aromatic ligands since it appears that the linearity of the ligand–Mn–ligand bond is distorted to a greater degree than are the complexes with alkyl ligands.[12] This apparent contradiction is discussed below.

The CN force constants for the Mn(II) complexes are greater than those in the Mn(I) complexes, demonstrating the loss of back-bonding in the Mn(II) complexes that accompanies the loss of a t_{2g} electron.

Table IV shows that the CN force constants are greater in the Mn(II) complex than in the corresponding free ligand. Cotton and Zingales[11] explained this observation by examining the valence-bond structures of the isocyanide ligands, structures I and II. They reasoned that the 2+ charge of the Mn(II) will enhance

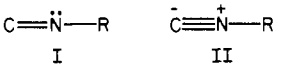

I II

the importance of II over I. Since the degree of back-donation is small for the Mn(II) complexes, the increased CN bond strength will lead to a higher CN frequency. Another explanation is that of Fenske and Sarapu.[5] On the basis of their calculations on CH_3NC, they observed that the isocyanide lone-pair orbital used in bonding to the metal has a slightly negative overlap population. This indicates a slight amount of antibonding in the CN region of the molecule, and any electron donation from this orbital will increase the CN bond strength. Our calculations (Table III) also indicate that there is a slightly negative overlap population between the C and N for all the isocyanides. We attribute the increase in frequency for the Mn(II) complexes relative to the free ligand to electron donation from the isocyanide lone pair.

In parallel with the change in the CN force constants described above, there should be a change in the MnC force contants, reflecting a variation in the back-bonding. The data in Table I do not show any trend. This can probably be attributed to the approximate method used in calculating the force constants. Use of eq 2 requires that the MnC vibration depend only on the mass of the isocyanide ligand and further requires that no intraligand vibrations exist with frequencies close to the MnC frequency. These requirements are met as long as the ligand behaves as a simple mass and the MnC vibration results in a movement of the entire ligand as if it were a large "atom". This will be true when the intraligand vibrations are at a high frequency compared to the MnC vibration. The assumptions become increasingly erroneous for the larger ligands.

Reduction potentials are a measure of the energy difference between reduced and oxidized species. Since the electron removed in an oxidation comes from the HOMO of the complex, it is possible in some cases to correlate $E_{1/2}$ values with the HOMO energy of the complex. Such a correlation has been found for the series $[Mn(CO)_n(CNCH_3)_{6-n}]^+$ (n = 0–6)[5] and also for a series of aromatic hydrocarbons.[24] Caution must be used in such correlations, however, because solvation and ion pairing can affect reduction potentials. Good donor solvents raise the potential of $Mn(CNCH_3)_6^{+/2+}$ compared to the same potential measured in poor donor solvents.[4] Less sterically hindered complexes should

Table V. Individual Atom Contributions to the π-Antibonding Orbital Wave Functions for Phenyl and *tert*-Butyl Isocyanides

		% character						
		C	N	C^1	$C^{2,6}$	$C^{3,5}$	C^4	all H
phenyl[a]	π_x^*	13.67	0.96	27.59	9.99	5.29	27.45	0.00
	π_y^*	41.84	21.08	3.28	10.58	5.07	0.00	2.50
		% character						
		C	N	C^1	C^2	C^3	C^4	all H
tert-butyl[b]	π_x^*	32.52	14.55	7.69	22.18	11.12	4.00	7.94
	π_y^*	32.52	14.55	7.69	2.38	13.84	21.02	8.00

[a]

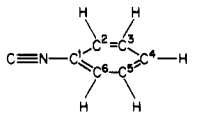

[b]

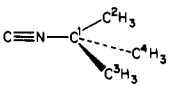

be more strongly influenced by this effect when it is present. The ion pairing necessarily present in solvents of low dielectric constant can also influence trends in redox potentials as observed by Mann and co-workers[25] in their studies of $Cr(CN(Ar))_6^{0/+/2+/3+}$, where Ar represents a variety of substituted phenyl groups. Ion pairing will also be enhanced for smaller, less hindered complexes.

The solvents for the electrochemical studies were chosen to vary both the dielectric constant and the Gutmann donor number, as shown in the footnotes to Table II. Conductivity experiments[1] have shown that in acetonitrile, and other solvents of relatively high dielectric constant, ion pairing is negligible under our conditions. However, in the lower dielectric solvents such as dichloromethane ion pairing is extensive. The trends we observe in $E_{1/2}$ values are independent of solvent. We conclude that the trend in reduction potentials is not due to solvent or ion-pairing effects but is an indicator of the energy of the HOMO of the complex, with a higher $E_{1/2}$ correlating with a more stable HOMO.

The trends in the force constant and the cyclic voltammetry data can be explained by the energy of the free-ligand antibonding orbitals. The trends in the force constants are due to a varying degree of back-bonding that depends on the similarity of the π^* and t_{2g} energies. In order to check these observations, we calculated the energies of the free-ligand orbitals, and as Table II indicates, the energies of the lowest level are not constant among the various ligands but decrease in the order methyl > *tert*-butyl > ethyl > isopropyl > cyclohexyl > benzyl > *p*-anisyl > *p*-tolyl > phenyl. Also, two antibonding MO's were obtained that were nearly constant in energy for the alkyl ligands but different for the aromatics. An explanation for the difference in energy for the aromatic MO's was given by Fenske and Bursten.[23] They showed that, for the stabilized MO, the wave function describing it had significant contribution from all the atoms in the molecule while, for the higher energy MO, the wave function was primarily localized about the CN region. Table V shows the wave function describing the π antibonding MO's broken down into contributions from individual atoms for the phenyl ligand and is representative of the other aromatic molecules including the benzyl ligand. These results show that the π_x^* orbital does have a significant contribution from all the atoms in the molecule while the π_y^* orbital is primarily localized about the CN region. The delocalized nature of the π_x^* MO seems to stabilize it with respect to the π_y^* orbital. Table V also shows the individual atom contributions to the antibonding wave functions for *tert*-butyl isocyanide. It is apparent

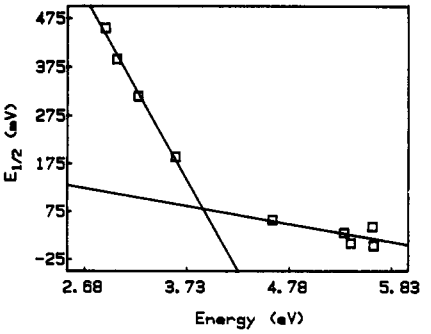

Figure 2. Plot of the reduction potential of the manganese isocyanide complexes vs. the energy of the ligand π^* orbitals. The large negative slope is for the aromatic complexes, and the other slope is for the alkyl complexes.

that both the π_x^* and π_y^* orbitals have primarily CN character and neither orbital is preferentially stabilized.

Of the two antibonding orbitals, the lower energy one will be favored for back-bonding. For the aromatic complexes the favored orbital will be the π_x^*, but for the alkyl complexes back-bonding will occur in both the π_x^* and π_y^* orbitals. The more comparable the energy of the favored MO is with the metal t_{2g} orbitals, the greater will be the back-bonding. Calculations on $Mn(CNCH_3)_6^+$ indicate that the energy of the metal t_{2g} orbitals is about −7 eV,[5] and Table III shows that the aromatic ligands have the MO's with energies closest to this. The aromatic complexes should therefore have the greater amount of back-bonding. However, recall from the data on the CN force constants that it appeared that the alkyl isocyanides were involved in a stronger back-bonding interaction than the aryl ligands. These apparently conflicting interpretations can be rationalized by considering the delocalized nature of the π_x^* orbital involved in back-bonding to the aryl isocyanides. For a given degree of back-bonding, the aryl ligands will show a much smaller change in the CN force constant because the electron density from the metal is delocalized around the ring and the CN group. For the alkyls, most of the electron density donated by the metal is localized on the CN group and has a much more profound influence on the CN force constant. Thus, the nature of the R group on the CN must be carefully considered when looking for evidence of back-bonding from just CN group frequencies in isocyanide complexes.

The smaller CN force constants in the aromatic ligands could be the result of coupling between the CN vibration and the vibrations within the aromatic ring. This would lower the vibrational frequency and the CN force constant, but we believe that such coupling is taken into account when comparing the Mn complex values to the free ligand values since the coupling should be approximately the same in the two.

Figure 2 shows a good correlation between the reduction potentials and the calculated energies of the ligand π-antibonding orbitals and, thus, the HOMO energies. Two slopes were obtained, corresponding to the aromatic and alkyl complexes, with the steeper slope being characteristic of the aromatic complexes. The correlation is excellent considering that we are estimating the HOMO energy of a transition-metal complex by calculating the electronic structure of the free ligand. The greater affect of the aryl ligands is consistent with the prediction that the back-bonding interaction is greater for these ligands.

The correlation of the ligand π^* energies with the CN force constants is not as good as with the reduction potentials and is probably due to the approximate methods used in calculating the force constants and the varying degree of C and N character to the total wave function describing the orbital used in back-bonding.

In conclusion, we have discussed the MnCNR bonding pattern in a series of $Mn(CNR)_6(BF_4)_{1,2}$ complexes. The trends in MnC and CN force constants and vibrational frequencies as well as the trend in $E_{1/2}$ values can be rationalized with the degree of back-bonding only if the delocalized nature of the ligand π^* orbital involved in the back-bonding of the aromatic isocyanides is considered. This delocalization is evident in the electronic structure

(25) Bohling, D. A.; Evans, J. F.; Mann, K. R. *Inorg. Chem.* **1982**, *21*, 3546.

calculated by an ab initio SCF method using the GAUSSIAN 76 programs.

Acknowledgment. The authors thank D. Borchardt for assistance with the electrochemistry, Professor K. Hipps for assistance in obtaining the Raman data, and Professor R. Poshusta and Dr. R. Knochenmuss for assistance with the GAUSSIAN 76 programs. This work was supported by National Science Foundation Grant CHE-8204-102.

Registry No. $Mn(CNCH_3)_6BF_4$, 91281-18-4; $Mn(CNCH_3)_6(BF_4)_2$, 95979-49-0; $Mn(CNC_2H_5)_6BF_4$, 91281-19-5; $Mn(CNC_2H_5)_6(BF_4)_2$, 95979-50-3; $Mn(CNC_3H_7)_6BF_4$, 95979-42-3; $Mn(CNC_3H_7)_6(BF_4)_2$, 95979-52-5; $Mn(CNC_4H_9)_6BF_4$, 95979-44-5; $Mn(CNC_4H_9)_6(BF_4)_2$, 95979-54-7; $Mn(CNC_6H_{11})_6BF_4$, 89463-46-7; $Mn(CNC_6H_{11})_6(BF_4)_2$, 89463-47-8; $Mn(CNCH_2C_6H_5)_6BF_4$, 95979-45-6; $Mn(CNCH_2C_6H_5)_6(BF_4)_2$, 95979-55-8; $Mn(CNC_6H_5)_6BF_4$, 95979-46-7; $Mn(CNC_6H_5)_6(BF_4)_2$, 95979-56-9; $Mn(CNC_6H_4CH_3)_6BF_4$, 95979-47-8; $Mn(CNC_6H_4CH_3)_6(BF_4)_2$, 95979-57-0; $Mn(CNC_6H_4OCH_3)_6BF_4$, 95979-48-9; $Mn(CNC_6H_4OCH_3)_6(BF_4)_2$, 95979-58-1.

Supplementary Material Available: Tables of atomic coordinates and π_x^* and π_y^* orbital wave functions and unpolarized Raman spectra (24 pages). Ordering information is given on any current masthead page.

Contribution from the Department of Chemistry,
University of Missouri—Columbia, Columbia, Missouri 65211

Reactions of WCl_2L_4 (L = a Phosphine). 2.[1] Tungsten(IV) and Tungsten(V) Hydride Complexes

PAUL R. SHARP* and KEVIN G. FRANK

Received August 22, 1984

Oxidative addition of H_2 to $WCl_2(PMe_3)_4$ gives quantitative yields of $WCl_2H_2(PMe_3)_4$ (**1**). Chloride can be removed from **1** by $AlCl_3$ or $TlBF_4$ to give $[WClH_2(PMe_3)_4]^+$ (**2**). In MeCN, the reaction of **1** with $TlBF_4$ gives $[WCl(MeCN)H_2(PMe_3)_4]^+$ (**3**). By NMR spectroscopy and cyclic voltammetry, **1** and **3** are found to be in equilibrium in MeCN ($K = 0.1$). Both **1** and **3** can be oxidized to $\mathbf{1}^+$ and $\mathbf{3}^+$, which are also in equilibrium ($K = 4 \times 10^{-6}$). Chemical oxidation of **1** can be accomplished with Ag^+ or $FeCp_2^+$, but only $\mathbf{1}^+$ is isolated. The oxidation of the BF_4^- salt of **3** in the absence of Cl^- gives $\mathbf{3}^+$. A crystal structure determination of a sample of $\mathbf{1}^+$, prepared with $FeCp_2BF_4$, was performed. The crystals are orthorombic (*Pbca*) with $a = 12.371$ (2) Å, $b = 19.328$ (8) Å, $c = 27.339$ (4) Å, $V = 6536.9$ (1) Å^3, and $Z = 8$. The three-dimensional X-ray data were measured with the θ–2θ scan technique with a scintillation detector. The structure was resolved by Patterson and Fourier methods and refined by full-matrix least-squares calculations to give $R(F_o) = 0.055$ and $R_w(F_o) = 0.062$ for 1733 observations above 2σ. The solid-state structure consists of monomeric cations and anions with ferrocene of crystallization. The hydride ligands were not located.

Introduction

The polyhydrides of molybdenum(IV) and tungsten(IV) have received attention for many years for reasons ranging from their fluxional behavior to their potential as reducing agents.[2-4] Simple high-yield preparations for these complexes are scarce. In addition, the majority of the members of this group are of the type MH_4L_4 (L = a phosphine). Cationic ($MH_xL_yL'z$; L' = MeCN) and neutral ($MX_2H_2L_n$; X = CF_3CO_2 or *p*-$MeC_6H_4SO_3$) derivatives have been prepared by reactions of the present hydrides, MH_4L_4, with various acids and solvents.[3,5-7] Another member, $WCl_2H_2(PMe_2Ph)_4$, has been prepared in low yield by reducing $WCl_4(PMe_2Ph)_3$ in THF with Mg.[8]

Recent attention has focused on improved preparations and attempts to prepare new members. Recently, an unsuccessful attempt to increase reactivity by oxidation of MoH_4L_4 to a paramagnetic molybdenum(V) hydride complex was reported.[3] (Few paramagnetic hydrides are known so their reactivity has not been fully explored.) In this paper we report the simple, high-yield preparation of $WCl_2H_2(PMe_3)_4$ (**1**), by simple oxidative addition of H_2 to $WCl_2(PMe_3)_4$. In addition, several derivatives of **1** can be readily obtained by halide abstraction. However, most interesting is the electrochemical behavior of **1** in MeCN: Two reversible one-electron-oxidation waves were observed, corresponding to the oxidation of **1** and its MeCN solvate, $[WCl(MeCN)H_2(PMe_3)_4]^+$ (**3**), to paramagnetic hydride complexes.

Scheme I

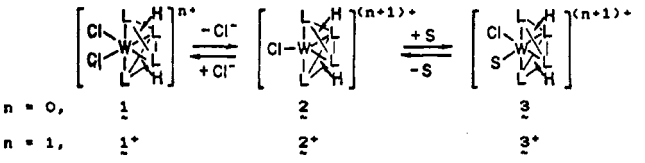

Results

Preparation and Characterization of $WCl_2H_2(PMe_3)_4$ (1). Orange $WCl_2(PMe_3)_4$ reacts readily with H_2 at 60 °C to give yellow $WCl_2H_2(PMe_3)_4$ (**1**; eq 1) quantitatively (96% isolated

$$WCl_2(PMe_3)_4 + H_2 \rightarrow \underset{\mathbf{1}}{WCl_2H_2(PMe_3)_4} \qquad (1)$$

yield). Unlike the related tetrahydrides, this diamagnetic complex is apparently static on the NMR time scale; two sets of phosphines and one set of hydrides are observed by ^{31}P and ^1H NMR spectroscopy, respectively. The spectra do not change between −50 and +70 °C, and simulation of the hydride region of the ^1H NMR spectrum indicated a rigid $HH'AA'B_2$ spin system (see Experimental Section and Supplementary Figure S-1a,b). These data are consistent with a dodecahedral geometry, the same geometry found for all other members of this group as well as the recently reported tantalum analogue of **1**.[9] An alternative and convenient, though not exact, description of this geometry is that of a distorted bi-face-capped octahedron. This representation of the structure of **1** is shown in Scheme I.

To further establish the presence of the hydride ligands, **1** was treated with $CDCl_3$. While a reaction did occur, little or no

(1) Part 1: Sharp, P. R. *Organometallics* **1984**, *3*, 1217-1223.
(2) Meakin, P.; Guggenberger, L. T.; Peet, W. G.; Muetterties, E. L.; Jesson, J. P. *J. Am. Chem. Soc.* **1973**, *95*, 1467-1474.
(3) Rhodes, L. F.; Zubkowski, J. D.; Folting, K.; Huffman, J. C.; Caulton, K. C. *Inorg. Chem.* **1982**, *21*, 4185-4192.
(4) Crabtree, R. H.; Hlatky, G. G. *Inorg. Chem.* **1982**, *21*, 1273-1275.
(5) Crabtree, R. H.; Hlatky, G. G.; Parnell, C. P.; Segmuller, B. E.; Uriarte, R. J. *Inorg. Chem.* **1984**, *23*, 354-358.
(6) Chiu, K. W.; Jones, R. A.; Wilkinson, G.; Galas, A. M. R.; Hursthouse, M. B.; Malik, K. M. A. *J. Chem. Soc., Dalton Trans.* **1981**, 1204-1211.
(7) Carmona-Guzzman, E.; Wilkinson, G. *J. Chem. Soc., Dalton Trans.* **1977**, 1716-1721.
(8) Fakley, M. E.; Richards, R. L. *Transition Met. Chem. (Weinheim, Ger.)* **1982**, *7*, 1.
(9) Luetkens, M. L., Jr.; Huffman, J. C.; Sattelberger, A. P. *J. Am. Chem. Soc.* **1983**, *105*, 4474-4475. Luetkens, M. L., Jr.; Elcesser, W. L.; Huffman, J. C.; Sattelberger, A. P. *Inorg. Chem.* **1984**, *23*, 1718-1726.

0020-1669/85/1324-1808$01.50/0